Case Report

Metastatic vertebral lesion mimicking an atypical hemangioma with negative 18F-FDG positron emission tomography-computed tomography

Lucas Paul Paladino, BS[a], Ana C. Belzarena, MD[b,], Evita Henderson-Jackson, MD[a], David M. Joyce, MD[a]*

[a] Sarcoma Department, Moffitt Cancer Center, 12902 Magnolia Dr., Tampa, FL, 33612, USA
[b] Orthopaedic Oncology Department, Miami Cancer Institute, 8900 N Kendall Dr., Miami, FL, 33176, USA

A B S T R A C T

Atypical hemangiomas of the spine can mimic metastatic lesions on magnetic resonance imaging, therefore making this distinction is a diagnostic challenge. In most cases, this conundrum can usually be solved with positron emission tomography/computed tomography images, because hemangiomas do not usually present with increased uptake while metastatic lesions do. Here we present a case of a patient with a unique diagnosis, myxoid liposarcoma, in which the vertebral metastatic lesion did not present with increased uptake in positron emission tomography/computed tomography scans. While keeping the imaging particularity of this rare sarcoma in mind, proceeding with a biopsy when the suspicion of metastasis remains high will help elucidate the diagnosis and allow for proper management.

Introduction

Intraosseous hemangiomas (IH) are benign vascular tumors which very rarely cause symptoms and are often found incidentally. Based on postmortem studies, it is estimated that they are found in 11% of the population [1]. IH most commonly occur between the fourth and sixth decade with a slight female predominance and 80% of cases will be localized to the skull or spine [2,3], where they are usually located in the vertebral body. Although they are most commonly found in the thoracic region, multiple locations can be present in up to

30% of cases [4,5]. IH have a classic radiologic appearance due to its histological content, which consists of a hamartomatous lesion with well-differentiated thin-walled vessels and a nonvascular component. The latter of which includes different percentages of fat, fibrous tissue, bone, hemosiderin, and smooth muscle [2,4]. The spatial arrangement of such components within the vertebral body translates into several classic radiologic findings. On radiographs, vertical striations and honeycomb appearance can be seen, while on computed tomography (CT) polka-dots are observed [6]. Magnetic resonance imaging visualizes IH as hyperintense T1-sequence lesions due to its lipomatous components and as hyperintense
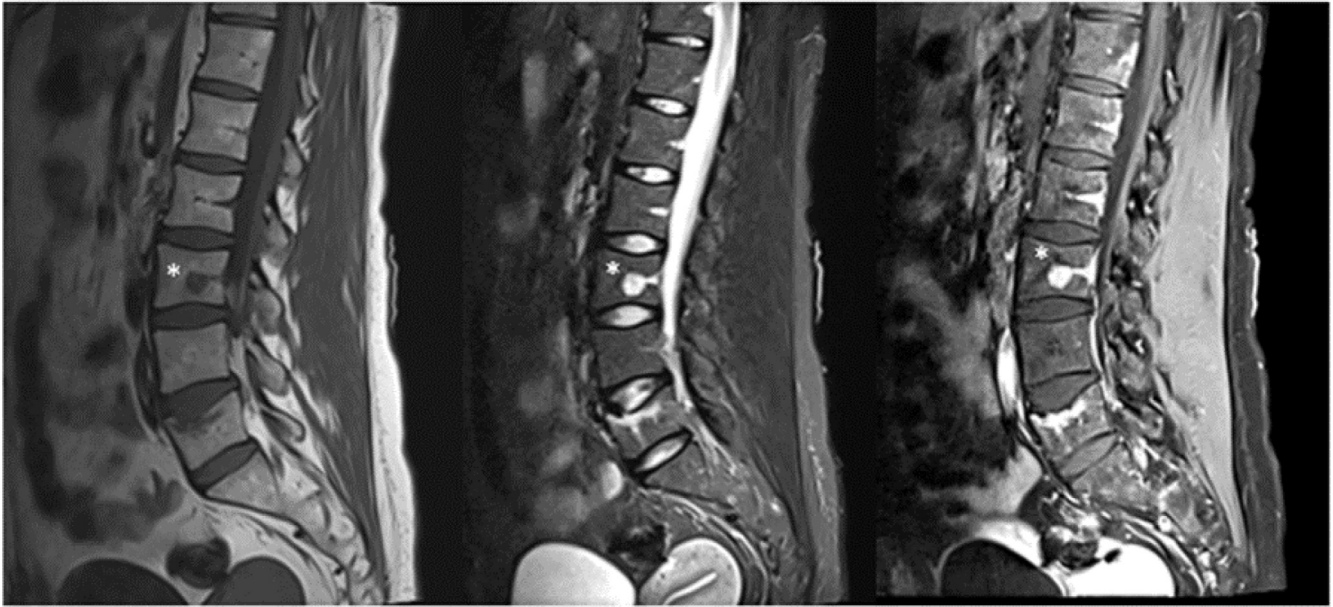
Fig. 1 – MRI of the lumbar spine (May 2018). Images depict findings consistent with a benign fracture and compression deformity of the superior endplate of L5 and a sharply marginated enhancing osseous lesion (*) in the L3 vertebral body. MRI, magnetic resonance imaging.

T2-sequence lesions due to the vascular portion, which also causes these lesions to be seen as enhancing under contrast administration [7–9]. On 18F-FGD positron emission tomography/CT (PET/CT) scans IH are visualized as cold lesions with no increased uptake above background. There have been some reported cases of increased uptake of rib hemangiomas and spine hemangiomas, however this is usually not the case [10–13].

An atypical hemangioma is a hemangioma that does not present with a classical imaging appearance and may resemble a more aggressive type of lesion [14]. Different distributions of tissue content within these lesions results in this idiosyncrasy. Atypical hemangiomas with low lipomatous percentage may present as hypointense on T1-sequence, but because of the lesion's vascular component, it can display T2-sequence hyperintensity with enhancement under contrast, thus resembling a metastatic lesion and clouding the difference between the 2 [15,16]. Adding to this diagnostic challenge, an atypical hemangioma may also present with aggressive features such as cortical destruction, bone expansion, and even invasion of the spinal canal. These are observations frequently associated with metastatic processes [2,17]. Prior studies have shown that new MRI techniques using diffusion weighted imaging combined with apparent diffusion coefficient maps and T1-weighted dynamic contrast-enhancing may help resolve this diagnostic problem, but unfortunately these techniques are not part of the standard of care [18,19].

Case report

A 31-year-old female with a history of a myxoid liposarcoma (MLS) excised from the left thigh, the primary location of the tumor, 2 years prior was under our care for a recurrent localized tumor with no evidence of other metastatic disease. The primary tumor presented on MRI as a soft tissue localized lesion hypointense in T1-weighted sequences, hyperintense in T2 with fat suppression ones and with heterogeneous enhancement with gadolinium contrast. She had received systemic treatment and awaited surgical resection and endoprosthetic reconstruction of this lesion. The patient presented to our clinic in May 2018, prior to her procedure, with acute back pain that developed during physical activity without any significant trauma. The pain was severe and included the lower back but did not have radiation to the lower extremities or any other neurologic findings. Radiographs of the lumbar spine obtained on that same date, showed an age indeterminate compression deformity of the L5 vertebral body involving the superior endplate, no signs of osteoporosis were noted. The radiographic image and the patient's symptoms prompted the acquisition of an MRI with and without gadolinium contrast, a week after the initial presentation, which confirmed a compression deformity and fracture of the L5 vertebral body, which could explain the patient's symptoms, and ruled out a neoplastic process at L5. Additional findings included a T1-sequnce hypointense and T2-sequence hyperintense lesion, enhancing under contrast in the L3 vertebral body with sharp margins. The lesion measured $1.24 \times 1.10 \times 0.93$ cm and was reported as potentially representing a metastatic lesion or an atypical vertebral body hemangioma (Fig. 1). A PET/CT scan was obtained 2 weeks after the initial presentation and showed increased uptake of the fractured L5 body but failed to show significant findings at the L3 vertebral body (Fig. 2). The case was presented at our sarcoma tumor board and we decided to delay the patient's femur resection and instead perform a CT-guided biopsy of the L3 vertebral body lesion as it would change surgical plan (Fig. 3). Histopathologic analysis of
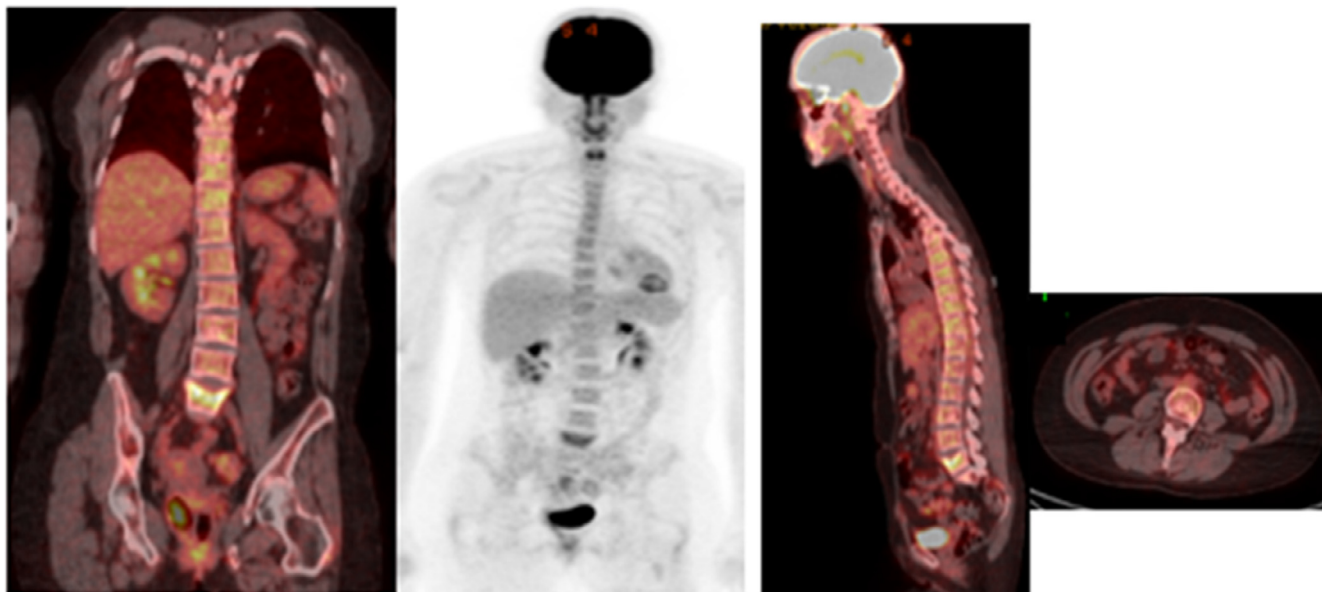
Fig. 2 – PET/CT (May 2018) showing increased uptake within the L5 vertebral body, related to moderate compression fracture deformity. No abnormal uptake in the L3 vertebral body. PET/CT, positron emission tomography/computed tomography.

Fig. 3 – CT images of the L3 vertebral body (May 2018), depicting the lesion's unspecific appearance (*) in a bone window (A), a soft tissue window (B) and the biopsy of the lesion with a percutaneous needle CT-guided technique (C).

the specimen obtained 3 weeks after the initial presentation, revealed a blood clot and medullary bone with no evidence of malignancy (Fig. 4). We later proceeded with her proximal femur resection and the preprocedure MRI showed no change in her L3 lesion at 2 months from the patient's presentation. The procedure was performed without complications and a margin-free resection was achieved.

Four months from the patient's initial presentation for acute back pain, a new PET/CT showed increased activity in the left medial thigh, a new large hypermetabolic left axillary lymph node, continued visualization of the L5 compression fracture, and no evidence of increased activity at L3. Work up of her left axillary lymph node verified metastatic spread of her MLS. After removal of this node, follow up PET/CT revealed a new mass in her left ovary, but again did not appreciate any significant findings at the L3 vertebral body at 7 months from presentation (Fig. 5). Although a pelvic MRI also at 7 months from the initial back pain symptoms, showed the ovarian mass was benign, we found that the L3 vertebral lesion's diameter had nearly tripled from 1.1 to 3.1cm and occupied the entire vertebral body (Fig. 6).
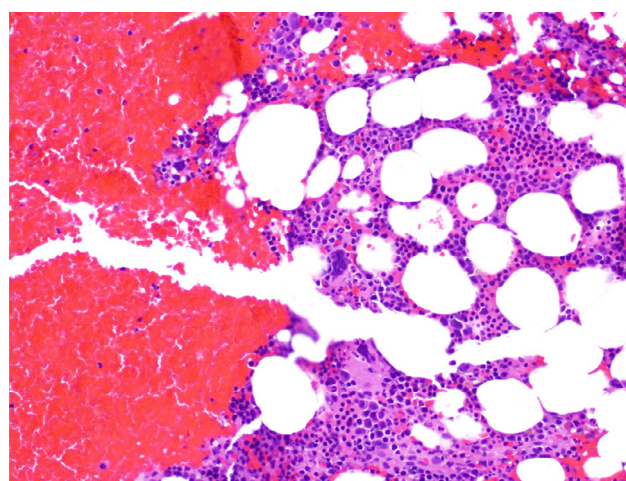

Fig. 4 – Percutaneous biopsy of L3 lesion pathology examination depicting normal bone marrow elements and blood (May 2018). No evidence of malignancy. [H&E, 20×].
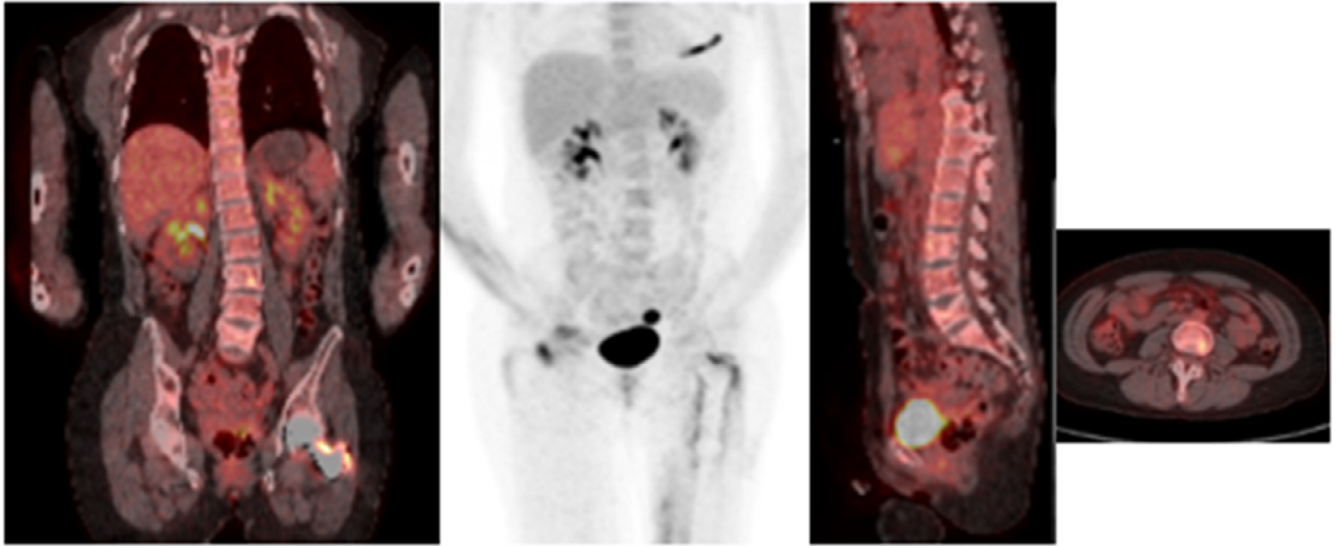
Fig. 5 – PET/CT (December 2018, post proximal femur resection) noted postoperative changes in the left thigh with a proximal femur reconstruction and a SUV maximum 3.4. No abnormal uptake at the L3 level. PET/CT, positron emission tomography/computed tomography.
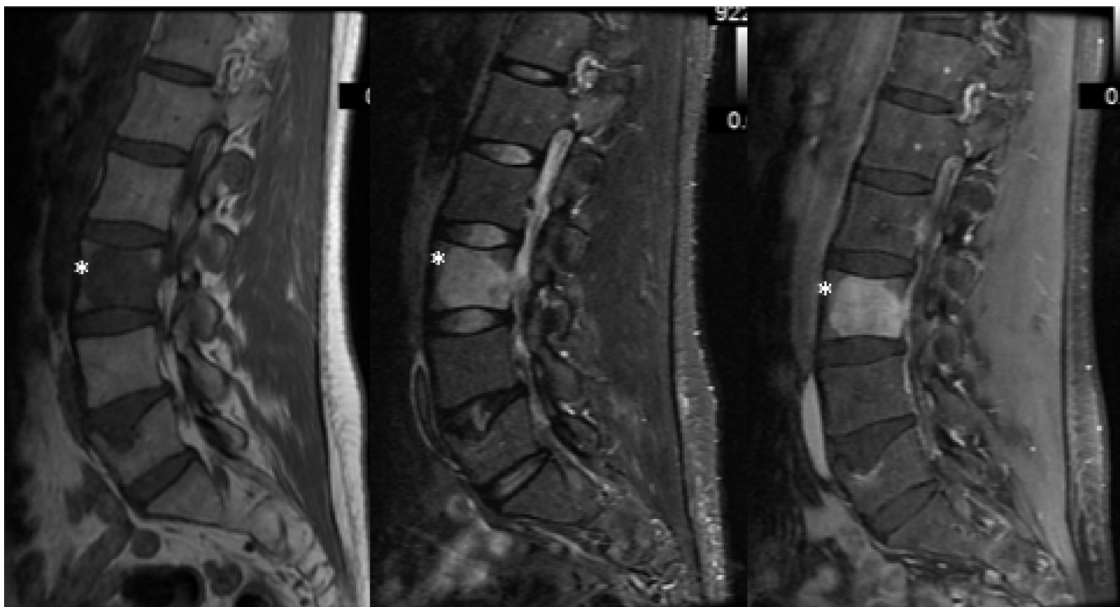

Fig. 6 – MRI of the lumbar spine (December 2018). The superior endplate fracture of L5 has healed. There is no evidence of underlying neoplastic disease. The marrow signal is normal at the L5 level. Interval increase in size of L3 lesion (*) from 1.1 cm in diameter to 3.1 cm. The lesion now extends from the superior to the inferior endplate and the posterior cortex to nearly the anterior cortex involving nearly the entire vertebral body. MRI, magnetic resonance imaging.

The sarcoma tumor board reviewed the patient's case again and now strongly suspected that the L3 lesion was a site of metastasis. Kyphoplasty and radiofrequency ablations were performed 7 months after presentation and a histopathologic sample obtained during the procedure confirmed this as a metastatic lesion of her primary MLS. A moderately cellular neoplasm with myxoid stroma, arborizing capillary vasculature, and spindled to round tumor cells with scant cytoplasm,

and hyperchromatic nuclei were observed in the sample with involvement of the bone marrow (Fig. 7).

The patient completed targeted lumbar radiation therapy. Follow up imaging of L3 almost a year from the initial symptoms has shown an increase in abnormal signal/marrow replacement, extending into the left pedicle and periphery of the vertebral body. Surveillance imaging has also discovered a new site in the left buttocks concerning for soft tissue
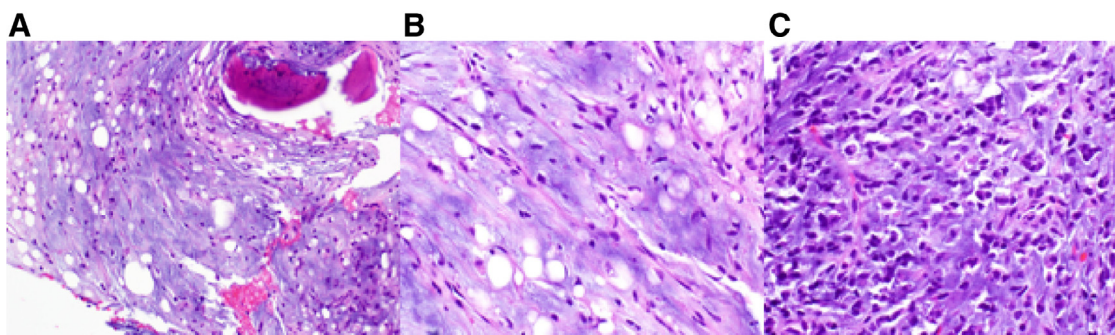
Fig. 7 – Open biopsy pathology images showing round to oval-shaped nonlipogenic cells and small lipoblasts embedded in a prominent myxoid stroma (December 2018) [H&E, 20 x] (A). High-power view of the round/oval nonlipogenic cells and small lipoblasts within myxoid stroma with delicate, branching vessels [H&E, 40 x] (B). High power view of focal area of increased cellularity with retention intercellular myxoid stroma [H&E, 40 x] (C).

metastasis. Now 32 years old, our patient is being evaluated for cellular therapy and a new systemic chemotherapy.

Discussion

Atypical hemangiomas and metastatic lesions, as previously mentioned, share common imaging features, such as signs of aggressiveness, similar patterns of intensity on T1 and T2 sequences, and enhancement seen on MRI [2,15–17]. They even present with similar age demographics: fourth to sixth decade for hemangiomas and fourth to fifth decades for MLS [2,26]. Both diagnoses should be considered a part of the differential, especially in patients with a known primary malignancy presenting with a vertebral lesion. More than 50% of the primary cancers will develop secondary bone lesions [20]. For many of these primary cancer types, studies have shown that PET/CT scans have a high specificity and sensitivity for detecting bone metastases when compared to other imaging modalities. Most tumor cells have increased glucose metabolism that causes the tracer to accumulate inside of these cells [21]. The majority of metastatic lesions analyzed with a PET/CT scan will display uptake, while typical and atypical hemangiomas usually have no increased signal. Therefore, PET/CT's are normally an important tool in differentiating metastases and hemangiomas.

However, in the case presented, the patient had a unique primary cancer type, MLS, which has many atypical and peculiar attributes, especially when it comes to PET/CT. MLS undergoes a different pattern of metastasis than other soft tissue malignancies. While most soft tissue cancers primarily spread to the lungs, MLS spreads more often to bone and lipomatous soft tissue in the retroperitoneum, axilla and mesentery, and classically the paraspinal muscles [22,23]. A third of MLS patients will progress to stage IV disease, with 14% of these patients having bone secondary lesions in a spine location [24]. The diagnosis of vertebral lesions secondary to MLS with 18F-FGD PET/CT or bone scintigraphy have shown low sensitivity, 14% and 16%, respectively [25], even though PET/CT are effective in highlighting primary and metastatic soft tissue sites of MLS. Schwab et al suggested that, in the setting of MLS,

myxoid stroma in the vertebral lesion potentially prevents labeled glucose from reaching cells in sufficient quantity to be detected by the scanner, thus accounting for such a low rate of detection by PET/CT [25]. The recommended method for detection of vertebral metastases, with the highest sensitivity, in the setting of MLS is the MRI [26].

If suspicion of metastasis remains high, it is recommended to proceed with a biopsy of the vertebral lesion and may even require and open biopsy. A prior study has shown a 10% rate of samples with insufficient material for histopathologic diagnosis with CT-guided biopsies of the spine, so having a pathologist to confirm the adequacy of sample on site can help lower this rate [27]. The overall accuracy for the diagnosis of spinal metastatic lesions with CT-guided biopsies ranges from 90% to 95% with a complication rate of <5% [28].

Conclusion

Atypical hemangiomas and MLS secondary spine lesions often present with many similar characteristics on MRI. While for most primary cancer types, PET/CT is useful in differentiating the 2, it is not helpful in the setting of MLS due to the tumor cell's reduced ability to absorb labeled glucose in the spine location. Here we presented this unusual scenario where an atypical hemangioma and metastatic process mimicked one another. Our patient had multiple negative PET/CT and no definitive MRI for over 6 months. It was not until an MRI, performed 2 weeks after a negative PET/CT, showed progression could we ultimately say there was a metastatic bone lesion. Ultimately, only an accurate biopsy confirmed metastatic spread to the vertebral body.

Sarcoma multidisciplinary treatment teams could face similar diagnostic challenges, analogous to the case presented. Making a distinction between a localized and a stage IV sarcoma has several implications in terms of treatment options and prognosis. In this case based on a questionable MRI with a negative PET/CT and negative biopsy the decision was made to proceed forward with resection and megaprosthetic reconstruction in the setting of previous radiation which has

significant risks associated. Consequently, it is paramount to arrive at a definitive diagnosis in the setting of MLS, utilizing MRI surveillance and biopsy when suspicion for metastasis is high.

Conflict of interest

The authors declare no conflict of interest.

REFERENCES

[1] Junghanns H, Schmorl G. The human spine in health and disease. New York: Grune & Stratton; 1971.

[2] McEvoy SH, Farrell M, Brett F, et al. Haemangioma, an uncommon cause of an extradural or intradural extramedullary mass: case series with radiological pathological correlation. Insights Imaging 2016;7:87–98.

[3] Wenger DE, Wold LE. Benign vascular lesions of bone: radiologic and pathologic features. Skeletal Radiol 2000;29(2):63–74.

[4] Murphey MD, Fairbairn KJ, Parman LM, et al. From the archives of the AFIP. Musculoskeletal angiomatous lesions: radiologic-pathologic correlation. Radiographics 1995;15:893e917.

[5] Vilanova JC, Barcelo J, Smirniotopoulos JG, et al. Hemangioma from head to toe: MR imaging with pathologic correlation. Radiographics 2004;24:367e85.

[6] Pessaaud T. The polka-dot sign. Radiology 2008;246(3):980–1.

[7] Baudrez V, Galant C, Vande Berg BC. Benign vertebral hemangioma: MR-histological correlation. Skeletal Radiol 2001;30:442–4.

[8] Laredo JD, Reizine D, Bard M, Merland JJ. Vertebral hemangiomas: radiologic evaluation. Radiology 1986;161(1):183–9.

[9] Ross JS, Masaryk TJ, Modic MT, et al. Vertebral hemangiomas: MR imaging. Radiology 1987;165:165e9.

[10] Dominguez M, Rayo J, Serrano J, et al. Vertebral hemangioma: ''cold'' vertebrae on bone scintigraphy and fluordeoxy-glucose positron emission tomography-computed tomography. Indian J Nucl Med 2011;26:49e51.

[11] Raphael J, Hephzibah J, Mani S, Shanthly N, Oommen R. Abnormal appearance of spinal hemangioma mimicking metastasis Mani S, Shanthly N, Oommen R. Abnormal appearance of spinal hemangioma mimicking metastasis in bone scintigraphy and SPECT CT: a case report. J Nucl Med Radiat Ther. 2013;S6:16–18.

[12] Itabashi T, Emori M, Terashima Y, Hasegawa T, Shimizu J, Nagoya S, Yamashita T. Hemangioma of the rib showing a relatively high 18F-FDG uptake: a case report with a literature review. Acta Radiol Open 2017;6(9):2058460117728416. doi:10.1177/2058460117728416.

[13] Nakayama M, Okizaki A, Ishitoya S, Aburano T. "Hot" vertebra on FDG PET scan; a case of vertebral hemangioma. Clin Nucl Med 2012;37(12):1990–3.

[14] Matrawy KA, El-Nekeidy AA, Gaber El-Sheridy H. Atypical hemangioma and malignant lesions of spine: can diffusion weighted magnetic resonance imaging help to differentiate? Egypt J Radiol Nucl Med 2013;44:259e63.

[15] Lakemeier S, Westhoff CC, Fuchs-Winkelmann S, et al. Osseous hemangioma of the seventh cervical vertebra with osteoid formation mimicking metastasis: a case report. J Med Case Rep 2009;3:92.

[16] Gaudino S, Martucci M, Colantonio R, et al. A systematic approach to vertebral hemangioma. Skeletal Radiol 2015;44:25–36.

[17] Pastushyn AI, Slin'ko EI, Mirzoyeva GM. Vertebral hemangiomas: diagnosis, management, natural history and clinicopathological correlates in 86 patients. Surg Neurol 1998;50:535e47.

[18] Morales KA, Arevalo-Perez J, Peck KK, Holodny AI, Lis E, Karimi S. Differentiating atypical hemangiomas and metastatic vertebral lesions: the role of T1-weighted dynamic contrast-enhanced MRI. AJNR Am J Neuroradiol 2018;39(5):968–73.

[19] Balliu E, Vilanova JC, Pelaez I, et al. Diagnostic value of apparent diffusion coefficients to differentiate benign from malignant vertebral bone marrow lesions. Eur J Radiol 2009;69:560e6.

[20] Du Y, Cullum I, Illidge TM, Ell PJ. Fusion of metabolic function and morphology:sequential [18F]fluorodeoxyglucose positron-emission tomography/ computed tomography studies yield new insights into the natural history of bone metastases in breast cancer. J Clin Oncol 2007;25:3440–7.

[21] Nakai T, Okuyama C, Kubota T, Yamada K, Ushijima Y, Taniike K, et al. Pitfalls of FDG-PET for the diagnosis of osteoblastic bone metastases in patients with breast cancer. Eur J Nucl Med Mol Imaging 2005;32:1253–8. doi:10.1007/s00259-005-1842-8.

[22] Antonescu CR, Elahi A, Humphrey M, Lui MY, Healey JH, Brennan MF, Woodruff JM, Jhanwar SC, Ladanyi M. Specificity of TLS-CHOP rearrangement for classic myxoid/round cell liposarcoma: absence in predominantly myxoid well-differentiated liposarcomas. J Mol Diagn 2000;2:132–8.

[23] Estourgie SH, Nielsen GP, Ott MJ. Metastatic patterns of extremity myxoid liposarcoma and their outcome. J Surg Oncol 2002;80(2):89–93. doi:10.1002/jso.1009.

[24] Schwab JH, Boland PJ, Antonescu C, Bilsky MH, Healey JH. Spinal metastases from myxoid liposarcoma warrant screening with magnetic resonance imaging. Cancer 2007;110:1815–22. doi:10.1002/cncr.22992.

[25] Schwab JH, Boland P, Guo T, Brennan MF, Singer S, Healey JH, Antonescu CR. Skeletal metastases in myxoid liposarcoma: an unusual pattern of distant spread. Ann Surg Oncol 2007;14:1507–14. doi:10.1245/s10434-006-9306-3.

[26] Sheah K, Ouellette HA, Torriani M, Nielsen GP, Kattapuram S, Bredella MA. Metastatic myxoid liposarcomas: imaging and histopathologic findings. Skeletal Radiology 2008;37(3):251–8.

[27] Gul SB, Polat AV, Bekci T, Selcuk MB. Accuracy of percutaneous CT-guided spine biopsy and determinants of biopsy success. J Belg Soc Radiol 2016;100(1):62.

[28] Filippiadis D, Mazioti A, Kelekis A. Percutaneous, imaging-guided biopsy of bone metastases. Diagnostics 2018;8(2):25.